An Electric-Circuit Model on the Inter-Tape Contact Resistance and Current Sharing for REBCO Cable and Magnet Applications

Aurora Cecilia Araujo Martínez, Qing Ji, Soren O. Prestemon, Xiaorong Wang, Georfrey Humberto I. Maury Cuna

***Abstract*—REBCO coated conductor has demonstrated high current capacity that can enable high-field magnets for high energy physics and fusion applications. However, quench protection is still one of the main challenges to be addressed for these applications. In addition, I_c and n value variations along the length of REBCO tapes exist in commercial production. The inter-tape contact resistance plays a key role to develop the self protection capability in cables and magnets by enabling current sharing and suppressing excessive eddy currents. Here we propose an electric-circuit model to describe the inter-tape contact resistance and its impact on the current sharing between REBCO tapes. We report the experiments on a 2-stacked tape REBCO cable with local I_c drop to validate the model. With the developed model, we study the upper limit of the contact resistance which allows current sharing between tapes. We also study the impact of variation in I_c and n values in tapes on the cable performance. Our model is expected to provide useful insight into the current sharing and target values for inter-tape contact resistance in REBCO cables and magnets for various applications.**

***Index Terms*—Contact resistance, current sharing, REBCO, stacked tape cable.**

I. Introduction

REBCO ($REBa_2Cu_3O_{7-\delta}$, RE = rare earth) coated conductor is a promising superconductor with multiple potential applications given its superior performance in high-field and high current capacity. Different cable configurations of REBCO, such as twisted stacked tape cable (TSTC) [1], Conductor on Round Core (CORC®) [2] and Symmetric Tape Round REBCO (STAR) wires [3], have been proposed for next generation high-field magnets for accelerators and fusion applications. REBCO pancake coils and layer wound coils have also been applied in Nuclear Magnetic Resonance (NMR) and Magnetic Resonance Imaging (MRI) [4], [5].

Although REBCO conductors can enable diverse high-field magnet applications, the REBCO conductor and magnet technology need to address several significant challenges. The protection against quench under a high engineering current density is an issue (100 - 1000 Amm^{-2}) [6]. Recent non-insulation (NI) REBCO magnet technology has demonstrated self-protection capability against quench and nominal operation regardless of defects by allowing current sharing between the conductor turns [7], [8], leading to a recent record DC field of 45.5 T [9]. Nevertheless, excessive eddy currents related to the low inter-tape contact resistance (R_c) in NI coils cause magnetic field distortions and charging/discharging delays [10], [11].

Another challenge is that critical current (I_c) and n value variations along the length of REBCO tapes exist in commercial tapes, which can cause non-uniform current distribution among the tapes in the cable, affecting the performance and reliable operation of cables and magnets [12]–[14].

The contact resistance between tapes plays a key role to determine the current distribution. Several models have been reported to understand the current distribution in REBCO cables. These models consider terminal resistances, tape inductances, and insulation between tapes [15]–[18]. It has been demonstrated that at steady-state conditions current sharing is determined by the terminal resistances for cables with insulation between tapes [19]–[22]. Different numerical methods and software have been implemented to analyze the electrical behavior of HTS cables [23]–[26].

In this paper, we report a simple electric-circuit model to analyze the impact of the contact resistance on current sharing between tapes with local I_c drops. We also study the impact of variation in I_c and n values on the transport performance of stacked tape cables. Our results can provide important insight into the role of inter-tape contact resistance on current sharing for REBCO cables and magnets.

II. Model of Stacked Tape Cable with Contact Resistance

We consider a cable composed of N REBCO tapes. Each tape can be divided into M sections that are represented by a voltage source $V_{i,j}$ (Fig. 1) following the power law,

$$V_{i,j} = V_c \left(\frac{I}{I_c}\right)^n, \tag{1}$$

where I_c is the critical current of the tape, n is the index value, and I the current flowing through the voltage source. V_c is the critical voltage LE_c, where L is the length of the tape and E_c is the electric field criterion of 100 μVm^{-1}. Both I_c and n value can vary along the tape and among the tapes.

Manuscript received on October 3, 2019. This work was supported by the Director, Office of Science, Office of High Energy Physics and Office of Fusion Energy Sciences of the U.S. Department of Energy under Contract No. DE-AC02-05CH11231.

A. C. Araujo Martínez, Q. Ji, S. O. Prestemon, and X. Wang are with Lawrence Berkeley National Laboratory, Berkeley, CA 94720. (E-mail: araujoma2012@licifug.ugto.mx).

A. C. Araujo Martínez and G. H. I. Maury Cuna are with University of Guanajuato, León, Gto., 37150, Mexico.

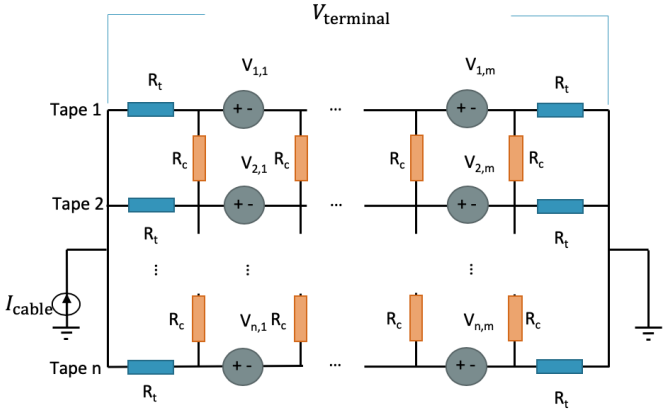

Fig. 1: A circuit model for stacked tape cable. REBCO tapes are divided into m sections represented by voltage sources $V_{i,j}$. Terminal resistances R_t and contact resistances R_c are included.

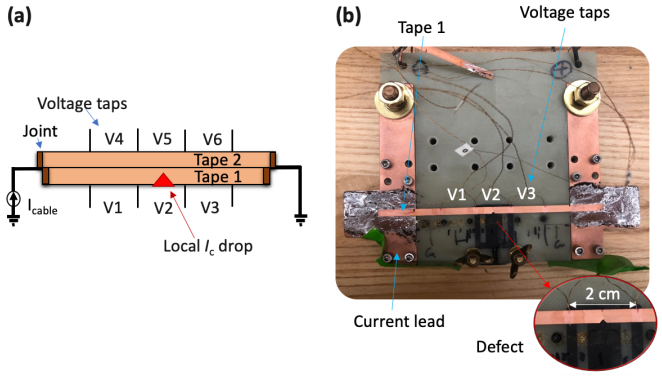

Fig. 2: 2-stacked tape cable with a local I_c drop. (a) Schematic of the cable (not to scale). (b) Experiment setup. We introduced the local I_c drop in the middle section of Tape 1 by making a small cut.

The model includes terminal resistances R_t at the ends of each tape, and contact resistances R_c between the tapes. All the tapes are connected to a current source I_{cable}. We use the open source NGSPICE [27], a circuit simulator based on the classic SPICE [28], to analyze the current and voltage distributions in the circuit model. The model can reproduce the results of measured and calculated current distributions on stacked tape cables [1], [15], [19].

III. Current Sharing in a 2-Stacked Tape Cable with a Local I_c Drop

To study the impact of R_c, let us consider a simple 2-stacked tape cable with a local I_c drop in one of the tapes. We studied the voltage and current distributions with two cases: low and high R_c.

A. Experiments

We used two 4 mm wide SuperPower tapes (SCS4050) to make the cable. The tape has a 50 μm thick Hastelloy® substrate and is surrounded by a 20 μm thick Cu stabilizer. Tape 1 was 13 cm long and Tape 2 was 4 cm longer, such that we could solder both tapes directly to the current leads using $Pb_{40}Sn_{60}$ solder. The substrate side of each tape was soldered directly to the terminals with 2 cm contact length at both ends. We soldered voltage taps separated by a distance of 2 cm in three sections on each REBCO tape. For Tape 1 these sections are labeled as V1, V2, and V3; for Tape 2 the corresponding sections are V4, V5, and V6 (Fig. 2). The voltage taps on Tape 1 were on the substrate side, whereas for Tape 2 they were on the REBCO side. The voltage taps were connected to nanovoltmeters to monitor the voltage. Another pair of voltage taps was soldered at the ends of Tape 2 to monitor the terminal voltage. We performed the following measurements:

1) Measure the I_c and n values for each tape separately at 77 K, self field.
2) Create a defect in Tape 1 by cutting a small portion in section V2. Measure the reduced I_c and n value at 77 K, self field.
3) Stack the tapes with a Kapton tape in between for insulation (high R_c). Solder the tapes to the current leads. Measure the voltage rise in all sections as a function of current.
4) Remove the Kapton tape and solder the two tapes together (low R_c). Solder the tapes to the current leads while maintaining the same contact surface as in Step 3. Measure the voltage rise in all sections as a function of current.
5) Un-solder the tapes and repeat Step 1.

During the measurements, the current was ramped in a stair-step way and the voltage across each section was only measured when the current ramping stopped to minimize the inductive voltage. The measured I_c and n values are shown in Table I. I_c and n *before* are the values measured in Step 1 for all sections except V2, for which they were measured in Step 2. I_c and n *after* are the results from Step 5 after the tapes were un-soldered. Fig. 4(a) shows the measured $V(I)$ data for the insulated case and Fig. 5(a) the $V(I)$ data for the soldered case.

TABLE I: Measured I_c and n values for each tape section. Before being soldered into a stacked tape cable and after desoldering from the stacked tape cable. The values for V1 and V3 could not be measured after creating a defect in section V2.

Tape	Section	I_c *before* (A)	I_c *after* (A)	n *before*	n *after*
Tape 1	V1	132	–	30.5	–
Tape 1	V2	89	87	24.2	24.4
Tape 1	V3	133	–	31.0	–
Tape 2	V4	133	130	28.9	28.8
Tape 2	V5	130	130	30.7	29.9
Tape 2	V6	132	129	29.7	28.3

B. Calculation

We applied the measured I_c and n values from Table I in the calculation. Fig. 3 shows the applied circuit model, which is a simplified case of the stacked tape cable model (Fig. 1) for two tapes with three sections each. The four contact resistances had the same constant value R_c. We did not consider the impact of the magnetic field on the I_c when both tapes are stacked. The terminal resistance $R_t = 1.29$ nΩ was determined from the measured terminal voltage before transition. We set $R_c = 1000$ Ω for the insulated case. For the soldered case, R_c was 46 nΩ based on the conductivity of the solder layer of 0.1 mm thickness (27 MSm^{-1} at 77 K [29]). The calculated voltages at the tape sections for high and low R_c are shown in Fig. 4(b) and Fig. 5(b). The current distribution through the tape sections and contact resistances are shown in Figs. 6 and 7. For the case of low R_c, the path of these currents is shown in Fig. 3. The power generated at the cable terminals and the section V2 for high and low R_c are shown in Fig. 8.

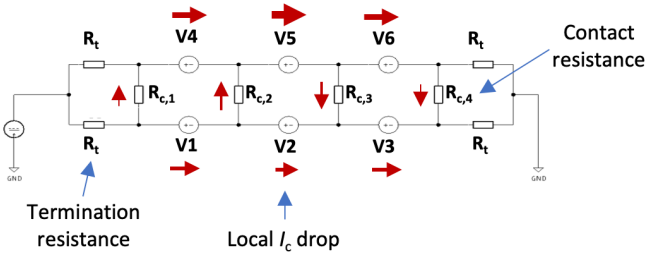

Fig. 3: Circuit model of a 2-stacked tape cable. The arrows show the current path for the case of low R_c. The size of the arrows indicates the amount of current (not to scale).

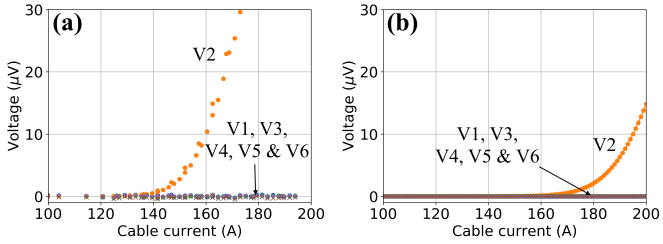

Fig. 4: Voltage at the tape sections with insulation (high R_c). (a) Measurement. (b) Calculation.

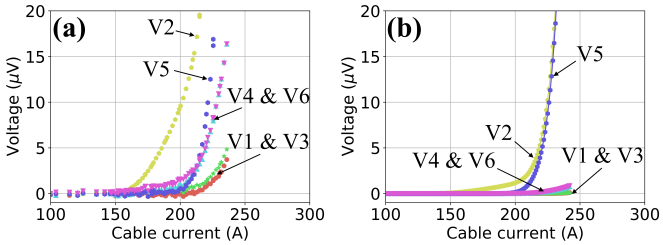

Fig. 5: Voltage at the tape sections with solder (low R_c). (a) Measurement. (b) Calculation.

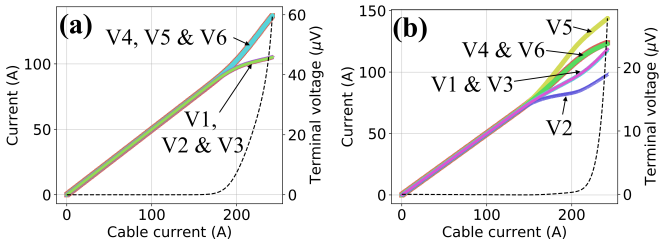

Fig. 6: Current through the tape sections. The dashed line is the terminal voltage with the resistive foot removed. (a) High R_c. (b) Low R_c.

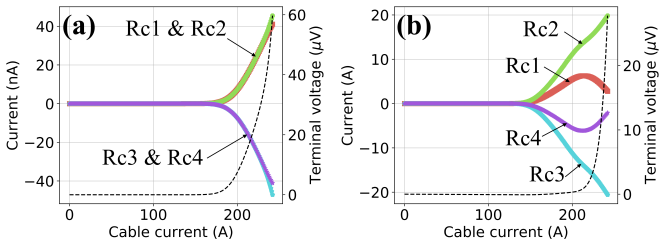

Fig. 7: Current distribution through the contact resistances. The dashed line is the terminal voltage with the resistive foot removed. (a) High R_c. (b) Low R_c.

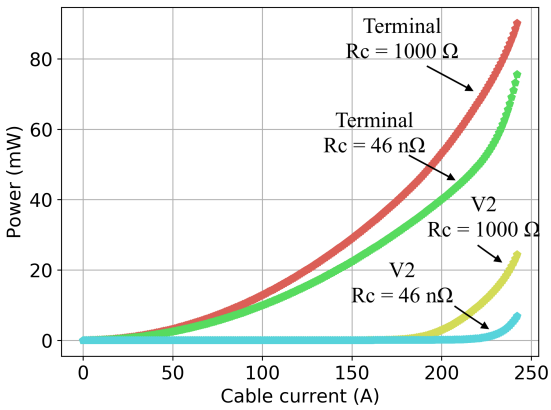

Fig. 8: Power generated at the cable terminals and the section V2 for high $R_c = 1000$ Ω and low $R_c = 46$ $n\Omega$.

IV. Upper Limit of R_c to Allow Current Sharing

The model presented here can also be used to determine the upper limit of R_c that allows current sharing. As an example, let us consider the 2-stacked tape cable model (Fig. 3). We assumed uniform I_c in each tape, having a value of 50 A in Tape 1 and 100 A in Tape 2. The n value was constant in all sections and equal to 30. The contact resistances $R_{c,i}$ were also uniform. We swept the R_c from 1 pΩ to 1000 Ω for three R_t values: 2.5 nΩ, 250 nΩ, and 25 $\mu\Omega$. We calculated the terminal voltage and the current distribution through the contact resistances as a function of current. Fig. 9 shows the results for $R_t = 250$ nΩ. The upper limit of R_c was selected in such a way that the terminal voltages and current distributions

for R_c values below this limit showed similar results. The upper limits of R_c to allow current sharing depending on R_t are shown in Table II.

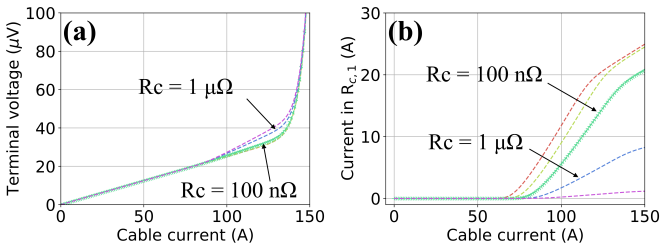

Fig. 9: Calculation results for various R_c in a 2-stacked tape cable with $R_t = 250$ nΩ. (a) Terminal voltage for different R_c. Voltages for $R_c < 100$ $n\Omega$ are overlapped. (b) Current through the contact resistance $R_{c,1}$.

TABLE II: Calculated upper limit of R_c to allow current sharing depending on R_t in a 2-stacked tape cable.

R_t	R_c upper limit
2.5 nΩ	1 nΩ
250 nΩ	100 nΩ
25 $\mu\Omega$	10 $\mu\Omega$

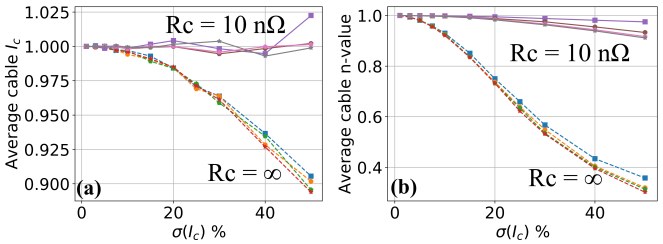

Fig. 10: Average cable parameters as a function of I_c variation for different number of tapes. $n = 30$ for all tapes. (a) Cable I_c. (b) Cable n value.

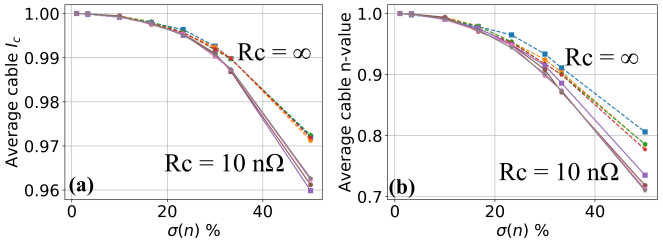

Fig. 11: Average cable parameters as a function of n value variation for different number of tapes. $I_c = 100$ A for all tapes. (a) Cable I_c. (b) Cable n value.

V. Impact of I_c and n value variation among the tapes of the stacked tape cable

We performed Monte Carlo simulations with sample size of 500 to study the impact of I_c and n value variation in the stacked tape cable model. The number of tapes ranges from 10 to 40. We analyzed two cases: high $R_c = \infty$ (open circuit) and low $R_c = 10$ nΩ. Tape I_c and n values were generated by normal distributions with a mean I_c of 100 A and a mean n value of 30. The standard deviations of I_c and n values were varied up to 50% of their mean values.

The terminal voltage V_{terminal} was calculated by sweeping the current up to 150% the cable I_c and time dependence was not considered. V_{terminal} was limited to 100 μV and fitted using (1) with $E_c = 100$ μVm^{-1} and $L = 1$ m to calculate the cable I_c and n value.

The cable I_c and n values for the 500 samples per each standard deviation were averaged and normalized to the results of 1% standard deviation. Figs. 10 and 11 show the results from the variations of I_c and n value.

VI. Discussion

Calculated voltage across each tape section qualitatively agreed with measurements in both insulation and solder cases. For high R_c only voltage in section V2 rose (Fig. 4). In contrast, for low R_c all sections showed voltage rise (Fig. 5), which is an indication of current sharing. There are several factors that can explain the discrepancy between the measurements and calculations: the actual values of R_c and R_t may be different from the values used in the calculation; the I_c reduction due to self-field effects in the stacked tape cable [30] was not considered; potential non-uniform I_c within each section can also contribute to the discrepancy. Although the I_c from each tape decreased by 3% after being soldered, the voltage rise in the soldered case (Fig. 5 (a)) was not caused by degradation of the tapes.

Low contact resistance allowed current to bypass the section with local I_c drop when approaching to its critical current (Figs. 3, 6(b), and 7(b)). Low R_c is necessary to decrease the power generation and the resulting temperature rise during the cable transition to normal state. For instance, with the low R_c the power was reduced by 26% at the cable terminals and by 90% at the section V2 when the cable current was 225 A (Fig. 8).

One important question is how low the contact resistance should be to allow current sharing. Our model can address this question by providing insight on the current distribution with different values of R_c (Fig. 9). For a simple 2-stacked tape cable, our model suggests that the R_c should be lower than 40% of the terminal resistance.

The simple circuit model presented here also allowed us to assess how the variation of I_c and n values in individual tapes affects the I_c and n value of the cable. With high R_c the cable I_c is less affected than the cable n value when the tape I_c or n value varies (Figs. 10 and 11). For example, a standard deviation of I_c of 30% only leads to 4% of cable I_c reduction, but it causes 50% drop in n value (Fig. 10). This result may also be interpreted as the following: if a cable with a high R_c between tapes shows a low n value (e.g. < 15, 50% of the mean value used in the model) this may indicate a strong I_c variation among the tapes.

We found that the cable I_c and n value were not affected by I_c variation when current can share between tapes through low R_c (Fig. 10). Hence, a low R_c between tapes benefits the cable performance by allowing current sharing, which is consistent with the observation in [8].

VII. Conclusion

We developed a simple circuit model to help understand the impact of contact resistance and current sharing for REBCO cables. The model can provide important insight of the relevance of the inter-tape contact resistance in REBCO cables. In particular, the benefits that low R_c brings to cable performance in the presence of defects.

The calculation qualitatively agreed with the measurements in a 2-stacked tape cable with solder or insulation between tapes. The current bypassed the section with lower I_c when the contact resistance was low. As a result, the power generation was lower compared to the case of high contact resistance. The model also gave insight on the current distribution for different R_c values. Reducing R_c will help the cable tolerate the variation of I_c in the tapes. We intend to include the self and mutual inductances between tapes to study the current sharing during non-steady state conditions.

Acknowledgment

We thank the technical support from Joe Walig and Timothy Bogdanof for the design and fabrication of the sample holder. We thank Arun Persaud for his guidance on NGSPICE. We also thank the useful discussions with Lucas Brouwer and Tengming Shen.

References

[1] M. Takayasu, L. Chiesa, L. Bromberg, and J. V. Minervini, "HTS twisted stacked-tape cable conductor," *Superconductor Science and Technology*, vol. 25, Art. no. 014011, Dec. 2011.

[2] D. C. van der Laan, J. D. Weiss, and D. M. McRae, "Status of CORC® cables and wires for use in high-field magnets and power systems a decade after their introduction," *Superconductor Science and Technology*, vol. 32, Art. no. 033001, Feb. 2019.

[3] S. Kar, W. Luo, A. B. Yahia, X. Li, G. Majkic and V. Selvamanickam, "Symmetric tape round REBCO wire with J_e (4.2 K, 15 T) beyond 450 A mm^{-2} at 15 mm bend radius: a viable candidate for future compact accelerator magnet applications," *Superconductor Science and Technology*, vol. 31, Art. no. 04LT01, Mar. 2018.

[4] C. Senatore, M. Alessandrini, A. Lucarelli, R. Tediosi, D. Uglietti, and Y. Iwasa, "Progresses and challenges in the development of high-field solenoidal magnets based on RE123 coated conductors," *Superconductor Science and Technology*, vol. 27, Art. no. 103001, Sep. 2014.

[5] H. Maeda and Y. Yanagisawa, "Recent developments in high-temperature superconducting magnet technology (review)," *IEEE Transactions on Applied Superconductivity*, vol. 24, pp. 1–12, June 2014.

[6] Y. Iwasa, *Case Studies in Superconducting Magnets*. Boston, MA: Springer, 2nd ed., Chapter 8, 2009.

[7] S. Hahn, D. K. Park, J. Bascunan, and Y. Iwasa, "HTS Pancake Coils Without Turn-to-Turn Insulation," *IEEE Transactions on Applied Superconductivity*, vol. 21, pp. 1592–1595, June 2011.

[8] S. Hahn, K. Radcliff, K. Kim, S. Kim, X. Hu, K. Kim, D. V. Abraimov, and J. Jaroszynski, "'Defect-irrelevant' behavior of a no-insulation pancake coil wound with REBCO tapes containing multiple defects," *Superconductor Science and Technology*, vol. 29, Art. no. 105017, Sept. 2016.

[9] S. Hahn, K. Kim, K. Kim, X. Hu, T. Painter, I. Dixon, S. Kim, K. R. Bhattarai, S. Noguchi, J. Jaroszynski, and D. C. Larbalestier, "45.5-tesla direct-current magnetic field generated with a high-temperature superconducting magnet," *Nature*, vol. 570, pp. 496–499, June 2019.

[10] X. Wang, T. Wang, E. Nakada, A. Ishiyama, R. Itoh, and S. Noguchi, "Charging Behavior in No-Insulation REBCO Pancake Coils," *IEEE Transactions on Applied Superconductivity*, vol. 25, pp. 1–5, June 2015.

[11] J. Lu, R. Goddard, K. Han, and S. Hahn, "Contact resistance between two REBCO tapes under load and load cycles," *Superconductor Science and Technology*, vol. 30, Art. no. 045005, Feb. 2017.

[12] V. Pothavajhala, C. H. Kim, L. Graber, and S. Pamidi, "Effects of Longitudinal Variations in Critical Current and n-Value of Individual Tapes on the Performance of Superconducting Cables," *IEEE Transactions on Applied Superconductivity*, vol. 25, pp. 1–4, June 2015.

[13] J. J. Gannon, A. P. Malozemoff, R. C. Diehl, P. Antaya, and A. Mori, "Effect of Length Scale on Critical Current Measurement in High Temperature Superconductor Wires," *IEEE Transactions on Applied Superconductivity*, vol. 23, Art. no. 8002005, June 2013.

[14] J. Kim, C. H. Kim, V. Pothavajhala, and S. V. Pamidi, "Current Sharing and Redistribution in Superconducting DC Cable," *IEEE Transactions on Applied Superconductivity*, vol. 23, Art. no. 4801304, June 2013.

[15] V. Pothavajhala, L. Graber, C. H. Kim, and S. Pamidi, "Experimental and Model Based Studies on Current Distribution in Superconducting DC Cables," *IEEE Transactions on Applied Superconductivity*, vol. 24, pp. 1–5, June 2014.

[16] A. D. Berger, "Stability of Superconducting Cables with Teisted Stacked YBCO Coated Conductors," Tech. Rep. RR-11-15, Plasma Science and Fusion Center, Massachusetts Institute of Technology, Cambridge, MA, Feb. 2012.

[17] F. Grilli, V. M. R. Zermeño, and M. Takayasu, "Numerical modeling of twisted stacked tape cables for magnet applications," *Physica C: Superconductivity and its Applications*, vol. 518, pp. 122 – 125, 2015.

[18] P. Krüger, V. M. R. Zermeño, M. Takayasu, and F. Grilli, "3-d numerical simulations of twisted stacked tape cables," *IEEE Transactions on Applied Superconductivity*, vol. 25, 2014.

[19] M. Takayasu, L. Chiesa, N. C. Allen, and J. V. Minervini, "Present Status and Recent Developments of the Twisted Stacked-Tape Cable Conductor," *IEEE Transactions on Applied Superconductivity*, vol. 26, pp. 25–34, Mar. 2016.

[20] G. P. Willering, D. C. van der Laan, H. W. Weijers, P. D. Noyes, G. E. Miller, and Y. Viouchkov, "Effect of variations in terminal contact resistances on the current distribution in high-temperature superconducting cables," *Superconductor Science and Technology*, vol. 28, Art. no. 035001, Jan. 2015.

[21] L. Bromberg, M. Takayasu, P. Michael, J. V. Minervini, and A. Dietz, "Current distribution and re-distribution in HTS cables made from 2nd generation tapes," (Spokane, Washington, USA), pp. 1001–1008, 2012.

[22] S. Venuturumilli, F. Berg, Z. Zhang, F. Liang, J. Patel, M. Zhang, and W. Yuan, "Forceful Uniform Current Distribution Among All the Tapes of a Coaxial Cable to Enhance the Operational Current," *IEEE Transactions on Applied Superconductivity*, vol. 27, pp. 1–4, June 2017.

[23] Z. Bai, W. Zu, C. Chen, and X. Zheng, "Modeling and numerical analysis of resistance network for non-insulated superconducting magnet," *Cryogenics*, vol. 60, pp. 19 – 23, 2014.

[24] P. C. Michael, L. Bromberg, D. C. van der Laan, P. Noyes, and H. W. Weijers, "Behavior of a high-temperature superconducting conductor on a round core cable at current ramp rates as high as 67.8 kA s^{-1} in background fields of up to 19 T," *Superconductor Science and Technology*, vol. 29, Art. no. 045003, Apr. 2016.

[25] V. M. R. Zermeño, P. Krüger, M. Takayasu, and F. Grilli, "Modeling and simulation of termination resistances in superconducting cables," *Superconductor Science and Technology*, vol. 27, Art. no. 124013, Nov. 2014.

[26] Y. Suetomi, K. Yanagisawa, H. Nakagome, M. Hamada, H. Maeda, and Y. Yanagisawa, "Mechanism of notable difference in the field delay times of no-insulation layer-wound and pancake-wound REBCO coils," *Superconductor Science and Technology*, vol. 29, Art. no. 105002, Aug. 2016.

[27] "Ngspice." (2018). [Online]. Available: http://ngspice.sourceforge.net.

[28] L. W. Nagel and D. Pederson, "Spice," April 1973. Available: http://www2.eecs.berkeley.edu/Pubs/TechRpts/1973/ERL-382.pdf.

[29] Y. Tsui, E. Surrey, and D. Hampshire, "Soldered joints—an essential component of demountable high temperature superconducting fusion magnets," *Superconductor Science and Technology*, vol. 29, Art. no. 075005, May 2016.

[30] W. Nah *et al.*, "Optimum reduction of self field effects in a Bi-2223 stacked superconducting busbar," *IEEE Transactions on Applied Superconductivity*, vol. 9, no. 2, pp. 960–963, June 1999.